Journal of The Electrochemical Society

OPEN ACCESS

An Analytical Approximation for the Ionomer Film Model in PEMFC

To cite this article: Thomas Jahnke and Andrea Baricci 2022 *J. Electrochem. Soc.* **169** 094514

Journal of The Electrochemical Society, 2022 **169** 094514

An Analytical Approximation for the Ionomer Film Model in PEMFC

Thomas Jahnke[1,z] and **Andrea Baricci**[2]

[1]*German Aerospace Center (DLR), Institute of Engineering Thermodynamics, Computational Electrochemistry, 70569 Stuttgart, Germany*
[2]*Politecnico di Milano, Dipartimento di Energia, 20156 Milano, Italy*

The ionomer film and its transport resistances for oxygen are considered to be an important aspect for PEMFC performance. Ionomer film sub-models are therefore frequently used in PEMFC modeling to account for this effect. Mathematically these are expressed by a non-linear equation for the oxygen concentration, which depending on the reaction order cannot be solved analytically. Typically, a numerical solution of this equation, e.g., using the Newton-method is needed. Here, we derive a highly accurate approximate analytical solution for the ionomer film model. This enables faster computation, which is particularly important for computationally demanding higher dimensional PEMFC models.
 [DOI: 10.1149/1945-7111/ac94a6]

Manuscript submitted June 2, 2022; revised manuscript received August 19, 2022. Published September 30, 2022.

Supplementary material for this article is available online

In PEMFC, oxygen needed for the ORR at the cathode has to be transported from the gas channels to the catalyst surface. Thereby, several transport resistances arise in the layered electrode structure (Fig. 1) due to multi-component diffusion within the GDL, Knudsen-diffusion within MPL and CL and diffusion through the ionomer film covering the platinum catalyst on the carbon support. In the literature the importance of the oxygen transport resistance due to the ionomer film has been reported by various authors, in particular for low platinum loadings[1–4] and in the course of catalyst degradation.[5,6]

A model describing the effect of the ionomer film on oxygen transport had been proposed by Secanell et al.[7,8] and later in a different form by Hao et al.[9] The ionomer film transport resistance can be caused by the diffusion through the ionomer film as well as additional resistances at the film interfaces.[8] For now, we do not specify the concrete form of this resistance, to stay as general as possible. In the discussion below, specific examples are provided. Calling the lumped total film resistance R_{film} the oxygen flux into the ionomer film covered carbon particle per platinum surface area can be written as

$$N_{O_2} = \frac{c_{O_2}^{\text{eq}} - c_{O_2}^{\text{Pt}}}{R_{\text{film}}} \qquad [1]$$

Here, the equilibrium concentration within the ionomer at the ionomer-gas interface is given by Henry's law

$$c_{O_2}^{eq} = H^{cc} c_{O_2}^{g}. \qquad [2]$$

In steady state this flux has to be equal to the amount of oxygen consumed by the ORR at the platinum surface according to Faraday's law

$$N_{O_2} = \frac{j_{ORR}(c_{O_2}^{\text{Pt}})}{4F}. \qquad [3]$$

Depending on the used model for the ORR kinetics, the specific current at the catalyst surface j_{ORR}, that depends on the local oxygen concentration at the catalyst active site ($c_{O_2}^{\text{Pt}}$), can be quite complex, e.g., when using a multi-step kinetics model.[10–12] In this case multiple intermediate species (e.g. O_{ad}, OH_{ad}) have to be taken into account whose coverages also depend on the oxygen concentration. However, Pant and Weber[13] have established a method to fit such a dependence to an effective kinetics with reaction order γ, i.e.,

$$j_{ORR} = 4F\tilde{r} = 4Fka_{\text{Pt}}^{\gamma} \qquad [4]$$

where $\tilde{r}$ is the specific reaction rate per catalyst active surface and the reaction rate constant k may include potential and temperature dependencies, dependencies on platinum oxide coverage etc. and the oxygen activity at the platinum surface is defined as $a_{Pt} = \frac{c_{O_2}^{\text{Pt}}}{C_{\text{ref}}}$.

Equating 1 and 3 using 4 yields the ionomer film equation, relating the oxygen concentration at the platinum surface with the equilibrium concentration

$$ka_{\text{Pt}}^{\gamma} + (a_{\text{Pt}} - a_{\text{eq}})\frac{C_{\text{ref}}}{R_{\text{film}}} = 0. \qquad [5]$$

In order to calculate the ORR reaction rate (4), Eq. 5 has to be solved for the oxygen concentration at the platinum interface a_{Pt}. In the general case, i.e., for arbitrary γ this cannot be done analytically. Instead (5) is usually solved numerically, e.g., using the Newton method. Such an iterative numerical method however leads to a higher computational cost, in particular in 2D or 3D models with complex geometries and up to several millions of grid points where this solution has to be obtained at every point within the cathode catalyst layer.[14] In the following, we derive an approximate analytical solution for the ionomer film model which yields high accuracy for arbitrary reaction orders in the range 0.5–1 as typically used in PEMFC models.

Theoretical.—We solve the problem in three steps: First, we propose a simple approximate solution for (5) which is exact in the two limiting cases $R_{\text{film}} \to 0$ and $k \to \infty$. Second, we calculate the maximum relative error of this first approximation. Finally, we construct a second improved approximation by introducing an appropriate correction term to the first approximation.

Equation 5 can be rewritten as equation for the reaction rate:

$$\tilde{r} = k\left(a_{\text{eq}} - \tilde{r}\frac{R_{\text{film}}}{C_{\text{ref}}}\right)^{\gamma}. \qquad [6]$$

Again, this equation generally cannot be solved analytically, except for a few particular choices of the reaction order γ.

[z]E-mail: thomas.jahnke@dlr.de

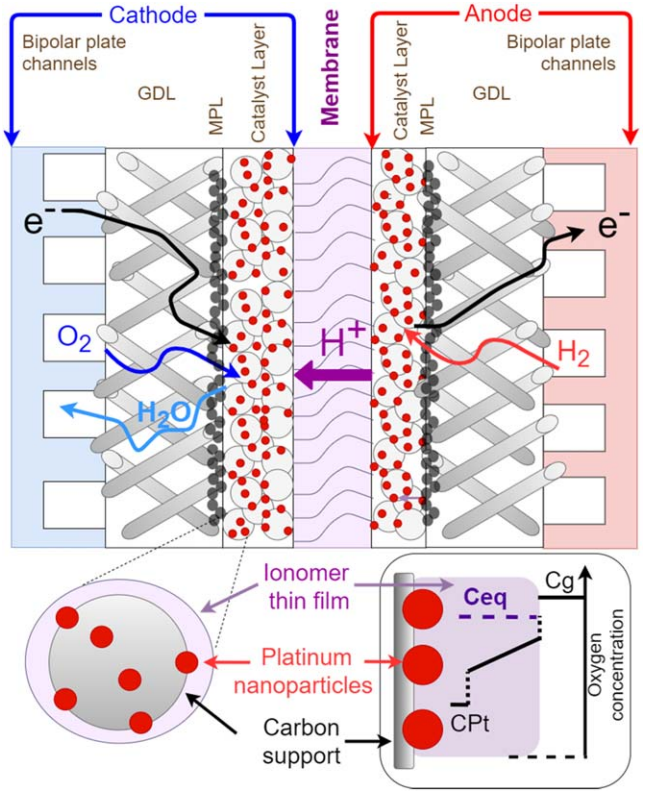

Figure 1. Graphical representation of the local oxygen transport resistance in the ionomer thin film that covers the supported platinum nanoparticles.

In case of $\gamma = 1$ we get the solution

$$\tilde{r} = k\frac{a_{eq}}{1 + \frac{1}{A}} \qquad [7]$$

with the dimensionless parameter $A: = \frac{C_{ref}}{k\, R_{film}}$ which represents the ratio between the kinetic and the thin film resistance.

For convenience we define $r: = \frac{\tilde{r}}{k}$, i.e., in the following r denotes the reaction rate divided by the rate constant. Accordingly, we define $r_{approx}: = \frac{\tilde{r}_{approx}}{k}$ for the approximate solution.

For arbitrary reaction order γ we propose the first approximate solution

$$\tilde{r}_{approx} = k\frac{a_{eq}^{\gamma}}{1 + \frac{a_{eq}^{\gamma-1}}{A}}. \qquad [8]$$

It can be easily seen that Eq. 8 gives the correct solution in the limiting cases, i.e., for $R_{film} \to 0$ we get $\tilde{r} = k a_{eq}^{\gamma}$ and for $k \to \infty$ we get the correct limiting reaction rate $r_{lim} = \frac{a_{eq} C_{ref}}{R_{film}}$. Furthermore, for $\gamma = 1$ Eq. 8 reduces to Eq. 7.

As next step, we derive an upper bound for the relative error of the approximate solution (8) in the general case.

From the definition of the relative error we get

$$\Delta r: = \frac{r - r_{approx}}{r} \Leftrightarrow r = \frac{r_{approx}}{1 - \Delta r}. \qquad [9]$$

First, we calculate the derivative of the reaction rate with respect to A

$$\frac{d}{dA} r = \frac{d}{dA}\left(a_{eq} - \frac{r}{A}\right)^{\gamma}. \qquad [10]$$

Using (9) we have

$$\frac{d}{dA} r = \frac{\frac{d}{dA} r_{approx}}{1 - \Delta r} + \frac{r_{approx}\frac{d}{dA}\Delta r}{(1 - \Delta r)^2}. \qquad [11]$$

At the point of maximum relative error $\frac{d}{dA}\Delta r = 0$, i.e., the last term vanishes. Thus, for the maximum relative error Eq. 11 can be rewritten as

$$\frac{d}{dA} r_{approx} = \gamma\left(a_{eq} - \frac{r_{approx}}{(1 - \Delta r_{max})A}\right)^{\gamma-1}\left(\frac{r_{approx}}{A^2} - \frac{\frac{d}{dA} r_{approx}}{A}\right). \qquad [12]$$

Substituting the approximate reaction rate as defined in (8) and its derivative

$$\frac{d}{dA} r_{approx} = \frac{a_{eq}^{2\gamma-1}}{\left(1 + \frac{a_{eq}^{\gamma-1}}{A}\right)^2 A^2} \qquad [13]$$

into Eq. 12 leads to

$$a_{eq}^{\gamma-1} = \gamma\left(a_{eq} - \frac{a_{eq}^{\gamma}}{\left(1 + \frac{a_{eq}^{\gamma-1}}{A}\right)(1 - \Delta r_{max})A}\right)^{\gamma-1}. \qquad [14]$$

Solving for the maximum relative error yields

$$\Delta r_{max} = \frac{a_{eq}^{1-\gamma} A \gamma^{\frac{1}{\gamma-1}} - a_{eq}^{1-\gamma} A - 1}{(1 + a_{eq}^{1-\gamma} A)\gamma^{\frac{1}{\gamma-1}} - a_{eq}^{1-\gamma} A - 1}. \qquad [15]$$

Using (15) we can calculate the reaction rate at the point of maximum relative error

$$r_{\Delta r_{max}} = \left(a_{eq} - \frac{r_{approx}}{(1 - \Delta r_{max})A}\right)^{\gamma} = \left(\frac{a_{eq}}{\gamma^{\frac{1}{\gamma-1}}}\right)^{\gamma}. \qquad [16]$$

Note, that this value only depends on the parameters a_{eq} and γ, while it is independent of A.

Next, we have to derive the relation between A and a_{eq} for which this maximum is reached. For this we evaluate the condition that the first derivative of Δr with respect to A has to vanish at $\Delta r = \Delta r_{max}$:

$$\begin{aligned}\frac{d}{dA}\Delta r|_{\Delta r = \Delta r_{max}} &= \frac{d}{dA}\left(\frac{r - r_{approx}}{r}\right)|_{\Delta r = \Delta r_{max}} \\ &= \frac{-\frac{dr_{approx}}{dA} r_{\Delta r_{max}} + r_{approx}\frac{\frac{dr_{approx}}{dA}}{1 - \Delta r_{max}}}{r_{\Delta r_{max}}^2} = 0 \\ \Rightarrow -r_{\Delta r_{max}} &+ \frac{r_{approx}}{1 - \Delta r_{max}} = 0. \end{aligned} \qquad [17]$$

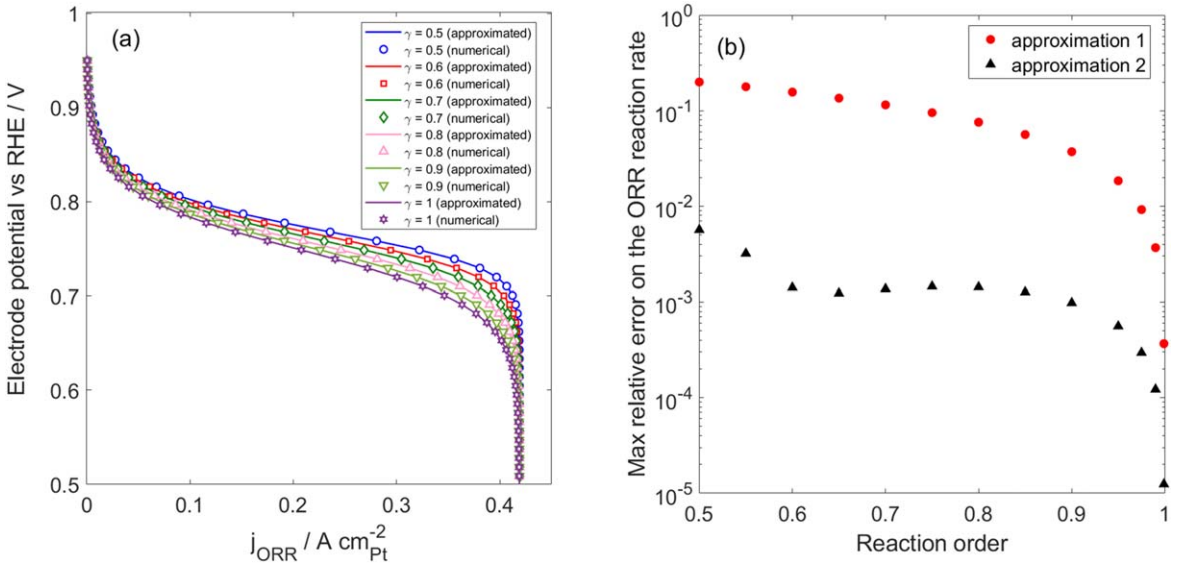

Figure 2. (a): Comparison of simulated polarization curves obtained from the exact numerical solution (symbol) and the derived analytical approximation (line) for reaction orders between 0.5 and 1. Other parameters used: $c_{O_2} = 13\,\frac{mol}{m^3}$ (corresponding to air at 2.3 bar and 100% RH); $T = 353.15\,K$;[4] $k = 7.72{\cdot}10^{-8}\frac{mol}{m^2_{Pt}\,s}$; $E_{act} = 42{\cdot}10^3\frac{J}{mol}$; $\alpha = 1$; $E_0 = 1.18\,V$; $R_{film} = 1200\frac{s}{m}$; $C_{ref} = 34.51\frac{mol}{m^3}$ (b) Maximum relative error, i.e., deviation from the numerically exact solution of the first approximation (8) (red symbols) and the improved approximation (21) (black symbols) depending on the reaction order.

Substituting (8), (15) and (16) in (17) and solving for A yields

$$A_{\Delta r_{\max}} = \frac{a_{\mathrm{eq}}^{\gamma-1}}{\gamma(\gamma^{\frac{1}{\gamma-1}} - 1)}. \qquad [18]$$

For convenience in the following we introduce

$$\tilde{A} := \frac{A_{\Delta r_{\max}}}{a_{\mathrm{eq}}^{\gamma-1}} = \frac{1}{\gamma(\gamma^{\frac{1}{\gamma-1}} - 1)}. \qquad [19]$$

Inserting (18) into (15) yields the final result for the maximum relative error of the first approximation

$$\Delta r_{\max} = \frac{\gamma^{\frac{1}{\gamma-1}} - \gamma^{\frac{\gamma}{\gamma-1}}}{(\gamma^{\frac{1}{\gamma-1}} - 1)\gamma^{\frac{\gamma}{\gamma-1}} + \gamma^{\frac{1}{\gamma-1}}}. \qquad [20]$$

Note, that this maximum error is independent of any parameters except for the reaction order γ.

Based on the calculation of the maximum error we can now propose the improved approximation

$$\tilde{r}_{\mathrm{approx},2} = k\frac{a_{\mathrm{eq}}^{\gamma}}{\left(1 + \frac{a_{\mathrm{eq}}^{\gamma-1}}{A}\right)\left(1 - 4\Delta r_{\max}\frac{A^b_{\Delta r_{\max}} A^b}{(A^b_{\Delta r_{\max}} + A^b)^2}\right)}. \qquad [21]$$

It can be easily seen that this kinetics still gives the correct solution in the limiting cases discussed above, i.e., for $R_{\mathrm{film}} \to 0$ and for $k \to \infty$.

Furthermore, it is constructed such that at $A = A_{\Delta r_{\max}}$ where the first approximation had the highest error the new approximation now gives the correct value

$$\tilde{r}_{\mathrm{approx},2}(A = A_{\Delta r_{\max}}) = k\frac{a_{\mathrm{eq}}^{\gamma}}{\left(1 + \frac{a_{\mathrm{eq}}^{\gamma-1}}{A_{\Delta r_{\max}}}\right)(1 - \Delta r_{\max})} = \tilde{r}(A = A_{\Delta r_{\max}}). \qquad [22]$$

The parameter b controls the width of the correction term. It can be shown (cf Supplementary Material) that the first and second derivative of the improved approximation at $A = A_{\Delta r_{\max}}$ are also identical to those of the exact solution if we choose

$$b = \frac{\sqrt{2}\sqrt{-2\tilde{A} + 2\tilde{A}\Delta r_{\max} - (\tilde{A} + 3\tilde{A}^2 + 3\tilde{A}^3 + \tilde{A}^4)(\Delta r_{\max} - 1)^2\beta}}{\sqrt{\Delta r_{\max}}(\tilde{A} + 1)} \qquad [23]$$

with

$$\beta = \frac{\gamma^{\frac{\gamma}{\gamma-1}}(\gamma - \gamma^2 + 2\gamma^{\frac{3}{\gamma-1}}(\gamma + 2\gamma^2) - 2\gamma^{\frac{1}{\gamma-1}}(\gamma - 2\gamma^2) - \gamma^{\frac{4}{\gamma-1}}(\gamma + \gamma^2) - 6\gamma^{\frac{2\gamma}{\gamma-1}})}{\gamma^{\frac{3\gamma+2}{\gamma-1}} + 3\gamma^{\frac{3}{\gamma-1}}(\gamma - 2\gamma^2 + \gamma^3) + \gamma^{\frac{2}{\gamma-1}}(1 - 3\gamma + 3\gamma^2 - \gamma^3) + 3\gamma^{\frac{4}{\gamma-1}}(\gamma^2 - \gamma^3)}. \qquad [24]$$

The correct first and second derivatives ensure that the approximation remains accurate over the whole parameter range of A.

Results and Discussion.—Equation 21 allows to calculate the reaction rate for the ionomer film model very efficiently. It should be noted that even though Eqs. 20 and 23 for the parameters $\Delta r_{\max}$ and b are quite complex they only depend on the reaction order and therefore only have to be calculated once at beginning of the simulation and can be considered as constants afterwards if the reaction order is constant. If the reaction order varies (e.g. with potential) our method is still applicable. In this case however to reduce the computational cost it might be beneficial to replace Eqs. 20 and 23 by the respective polynomial fits

$$\Delta r_{\max} \approx 0.0731865\ \gamma^2 - 0.508666\,\gamma + 0.435727; \qquad [25]$$

$$b \approx -0.42726\ \gamma^3 + 1.32779\ \gamma^2 - 1.6024\,\gamma + 1.59543. \qquad [26]$$

The proposed approximation (21) has a very high accuracy with its relative error being significantly lower compared to the first approximation (8) as shown in Fig. 2b. In the range of reaction

orders typically considered in PEMFC models this maximum relative error is about 0.1% and only depends on the reaction order.

Up to now we kept the discussion as general as possible and did not specify the actual form of R_{film}. The film resistance R_{film} can be calculated depending on the involved processes and the considered geometry. For example, for a planar ionomer film of thickness δ and taking into account diffusion through the film as well as interfacial resistances at the gas-ionomer and platinum-ionomer interfaces, we could write

$$R_{\text{film}} = \left(R_{\text{ext}} + \frac{\delta}{D} + R_{\text{int}} \right) \qquad [27]$$

Instead, following[7] for spherical ionomer film covered carbon particles of radius r with finite oxygen dissolution kinetics k_{O_2} and oxygen diffusion through the ionomer film we obtain

$$R_{\text{film}} = \frac{A_{\text{Pt}}}{4\pi(r+\delta)^2} \left[\frac{1}{k_{O_2}} + \frac{\delta}{D} \frac{(r+\delta)}{r} \right] \qquad [28]$$

where A_{Pt} is the platinum active surface area over a single carbon particle.

To demonstrate the accuracy of the derived approximation in a concrete example, Fig. 2a shows a comparison of the polarization curves obtained from solving Eq. 5 numerically and using the analytical approximation (21), where the specific current densities are calculated from the respective reaction rates according to Eq. 4 and the reaction kinetics in this example is defined as

$$k = k_0 e^{-\frac{E_{\text{act}}}{R}\left(\frac{1}{T} - \frac{1}{353.15\ K}\right)} e^{-\frac{\alpha F(\Delta\phi - E_0)}{RT}}. \qquad [29]$$

A very good agreement between numerical and analytical solutions is obtained, demonstrating that for all practical purposes the approximation is basically indistinguishable from the numerically exact solution. A Matlab script with an implementation of the analytical solution is provided as Supplement to the article.

Conclusions.—We have derived an approximate analytical solution for the ionomer film model with high accuracy. The analytical solution allows for a fast calculation of the reaction kinetics in the presence of an ionomer film resistance, which can be very beneficial especially in higher dimensional PEMFC models, where the ionomer film equation has to be solved locally at every point within the catalyst layer and coupled with all other relevant mechanisms such as two-phase, charge and energy transport. Having an analytical expression in this case can reduce significantly the computational cost compared to the alternative of numerically solving the respective ionomer film model equation. The presented solution is independent of the concrete formulation of the ORR kinetics or of the involved transport resistances of the ionomer film and therefore can be applied for a wide range of PEMFC models.

Acknowledgments

The research leading to these results has received funding from the European Union's Horizon 2020 research and innovation program under grant agreement no. 779565.

ORCID

Thomas Jahnke https://orcid.org/0000-0003-2286-6801
Andrea Baricci https://orcid.org/0000-0003-2331-7222

References

1. W. Yoon and A. Z. Weber, "Modeling low-platinum-loading effects in fuel-cell catalyst layers." *J. Electrochem. Soc.*, **158**, B1007 (2011).
2. A. Kongkanand and M. F. Mathias, "The priority and challenge of high-power performance of low-platinum proton-exchange membrane fuel cells." *J. Phys. Chem. Lett.*, **7**, 1127 (2016).
3. R. K. F. Della Bella, B. M. Stühmeier, and H. A. Gasteiger, "Universal correlation between cathode roughness factor and H_2/air performance losses in voltage cycling-based accelerated stress tests." *J. Electrochem. Soc.*, **169**, 044528 (2022).
4. T. A. Greszler, D. Caulk, and P. Sinha, "The impact of platinum loading on oxygen transport resistance." *J. Electrochem. Soc.*, **159**, F831 (2012).
5. S. Jomori, N. Nonoyama, and T. Yoshida, "Analysis and modeling of PEMFC degradation: effect on oxygen transport." *J. Power Sources*, **215**, 18 (2012).
6. G. S. Harzer, J. N. Schwämmlein, A. M. Damjanović, S. Ghosh, and H. A. Gasteiger, "Cathode loading impact on voltage cycling induced PEMFC degradation: a voltage loss analysis." *J. Electrochem. Soc.*, **165**, F3118 (2018).
7. M. Secanell, A. Putz, S. Shukla, P. Wardlaw, M. Bhaiya, L. Pant, and M. Sabharwal, "Mathematical modelling and experimental analysis of thin, low-loading fuel cell electrodes." *ECS Trans.*, **69**, 157 (2015).
8. A. Kosakian, L. Padilla Urbina, A. Heaman, and M. Secanell, "Understanding single-phase water-management signatures in fuel-cell impedance spectra: a numerical study." *Electrochimica Acta*, **350**, 136204 (2020).
9. L. Hao, K. Moriyam, W. Gu, and C.-Y. Wang, "Modeling and experimental validation of pt loading and electrode composition effects in PEM fuel cells." *J. Electrochem. Soc.*, **162**, F854 (2015).
10. K. Kudo, R. Jinnouchi, and Y. Morimoto, "Humidity and temperature dependences of oxygen transport resistance of nafion thin film on platinum electrode." *Electrochimica Acta*, **209**, 682 (2016).
11. J. X. Wang, J. Zhang, and R. R. Adzic, "Double-trap kinetic equation for the oxygen reduction reaction on Pt(111) in acidic media." *J. Phys. Chem. A*, **111**, 12702 (2007).
12. M. Moore, A. Putz, and M. Secanell, "Investigation of the ORR using the double-trap intrinsic kinetic model." *J. Electrochem. Soc.*, **160**, F670 (2013).
13. L. M. Pant and A. Z. Weber, "Modeling polymer-electrolyte fuel-cell agglomerates with double-trap kinetics." *Journal of The Electrochemical Society*, **164**, E3102 (2017).
14. B. Jayasankar and K. Karan, "O_2 electrochemistry on Pt: a unified multi-step model for oxygen reduction and oxide growth." *Electrochim. Acta*, **273**, 367 (2018).